

Figure 2.68. Framework for development of socio-economic and embedded landscape evolution scenarios. Inner boxes represent the landscape scenarios and outer boxes the social development contexts. These are arranged along axes of overall tree abundance and spatial distribution. "More patchy" implies that forest patches are more contiguous and distinct from other land-uses, whereas "Less patchy" implies smaller or less distinct patches with trees. A second pair of axes describing variation in social economic development can be overlaid on this framework to emphasize how the 4 scenarios differ with respect to social organization (Figure 2.69).

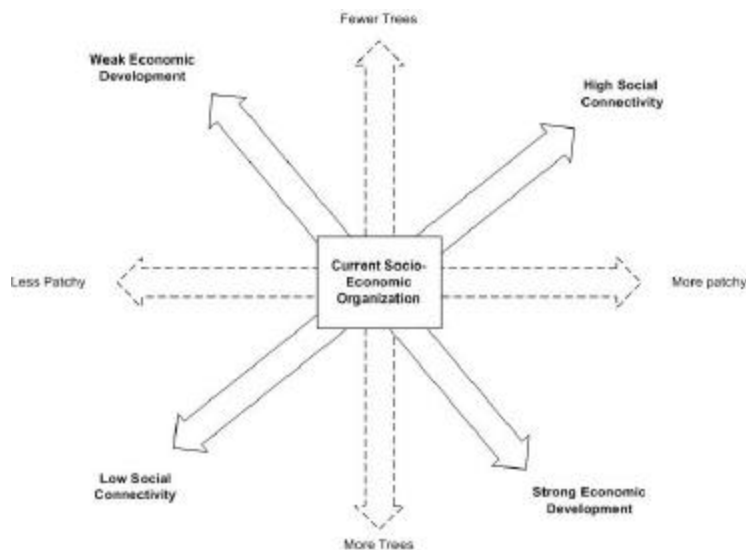


Figure 2.69. Key axes variation in landscape and social organization in the proposed scenario set. Levels of trade and the spatial extent of institutional arrangements are examples of social connectivity.

	Development Fixes	Globalization	Compartmentalized Growth	Localization
Economic Growth	→	↷	↗	↗
Tree Cover	↷	↷	↗	↗
Natural Biodiversity	↘	↘	↷	↷
Median Size of Tree Cover Patches	↷	↷	↷	↷
Proportion of Water Resources Used	→	↷	↷	→
Proportion of Water Resources Used	→	↷	↷	→

Figure 2.70. Underlying assumptions in the higher-scale scenarios about the shape of development trends and a few basic ecological and landscape indicators. Time frame of the x-axis in each panel is assumed to be from present out approximately 50 years.

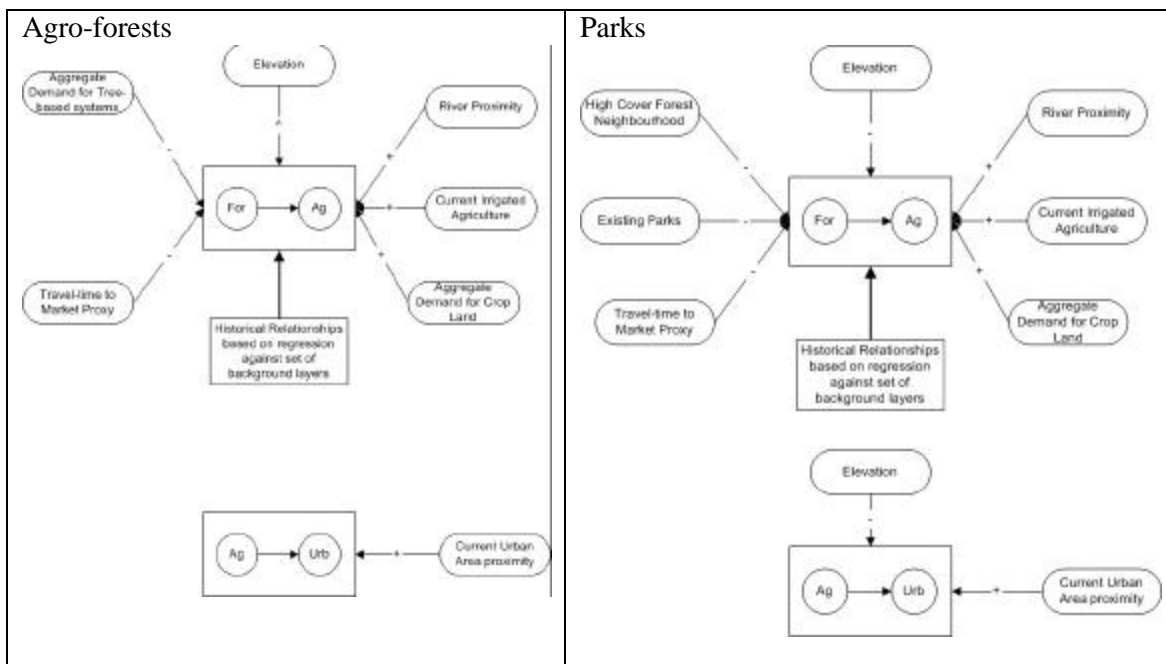


Figure 2.71. Conceptual models for evolving land-use in two of the scenarios.

3. Results

3.1 Analysis of the empirical data sets

3.1.1 Mae Chaem and Way Besai primary data

A graphical display of multi-year data on rainfall and river flow for Mae Chaem and Way Besai shows interesting patterns and lays the foundation for further analysis.

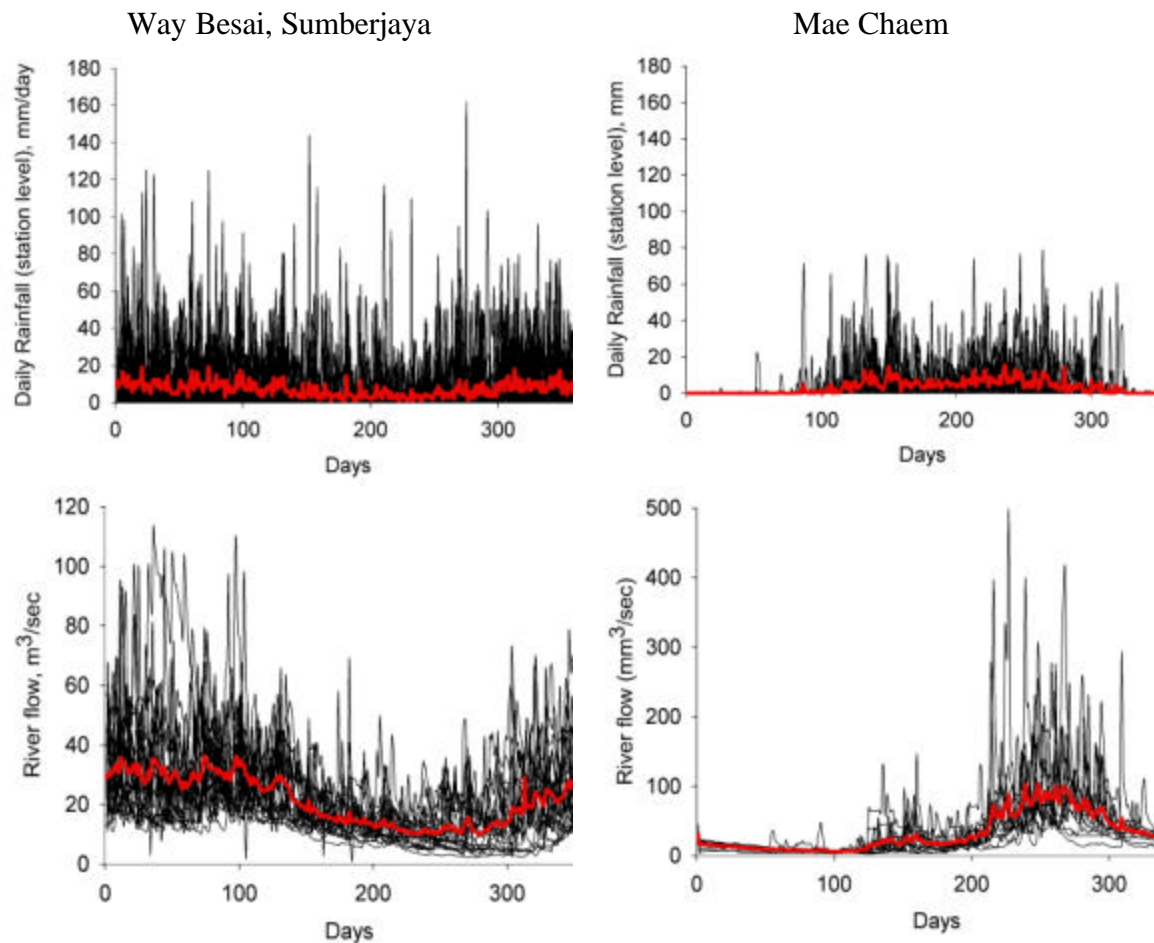


Figure 3.1. The records of the discharge and rainfall of the Way Besai for the 1975-1998 period (left; the red line indicates the mean daily discharge over data period) and Mae Chaem for the 1988-2000 (right); at least some of the downward spikes in river flow in the Way Besai record may reflect ill-functioning measurement equipment

We see the seasonal pattern of Mae Chaem reflected in both rainfall and river discharge, while Way Besai has only a mild seasonal difference. The maximum daily amounts of rainfall for Way Besai reach almost twice as high as those for Mae Chaem, but otherwise a re-scaled version of the 6 wettest months in Mae Chaem would fit well into the Way Besai record. The main difference thus is in the 'dry season', not so much in the rains during the 'rainy season'. When we consider the river discharge data for Mae Chaem in relation to the rainfall, we see that during the first half of the rainy season river flow is a much smaller fraction of rainfall than in the second half. Apparently the

catchment is making up for a water deficit from the dry season, before it conveys the rainfall on to the streams.

The peak river discharge for Mae Chaem reaches $500 \text{ m}^3 \text{ s}^{-1}$, while that for the Way Besai is $110 \text{ m}^3 \text{ s}^{-1}$. If we express both per unit area, however, the values amount to 11.0 and 13.6 mm day^{-1} , respectively -- remarkably similar, and only 12 or 9%, respectively, of the peak station-level rainfall record. There are, of course, a number of problems with this analysis, that require further analysis:

- The station-level rainfall records cannot be directly extrapolated to the whole catchment area (esp. for a property such as the maximum),
- The peak river flow record does not coincide in time with the peak rainfall record in either of the data sets,
- The statistical distributions of both rainfall and river discharge are clearly skewed, so statements about means and extremes need to be made with care.

We will have a closer look at the frequency distributions as such.

3.1.2 Mae Chaem 1988 - 2000

There is a statistically significant relationship (Fig. 3.2) between annual river discharge and annual rainfall at the Mae Chaem station, with an estimated slope of 30% and an intercept at 356 mm of rainfall. Mean discharge is 21% of the mean Mae Chaem station-level rainfall, while there is some indication of a positive relationship between this fraction and the annual rainfall, in line with the intercept. There was no significant trend with time for either rainfall or river flow.

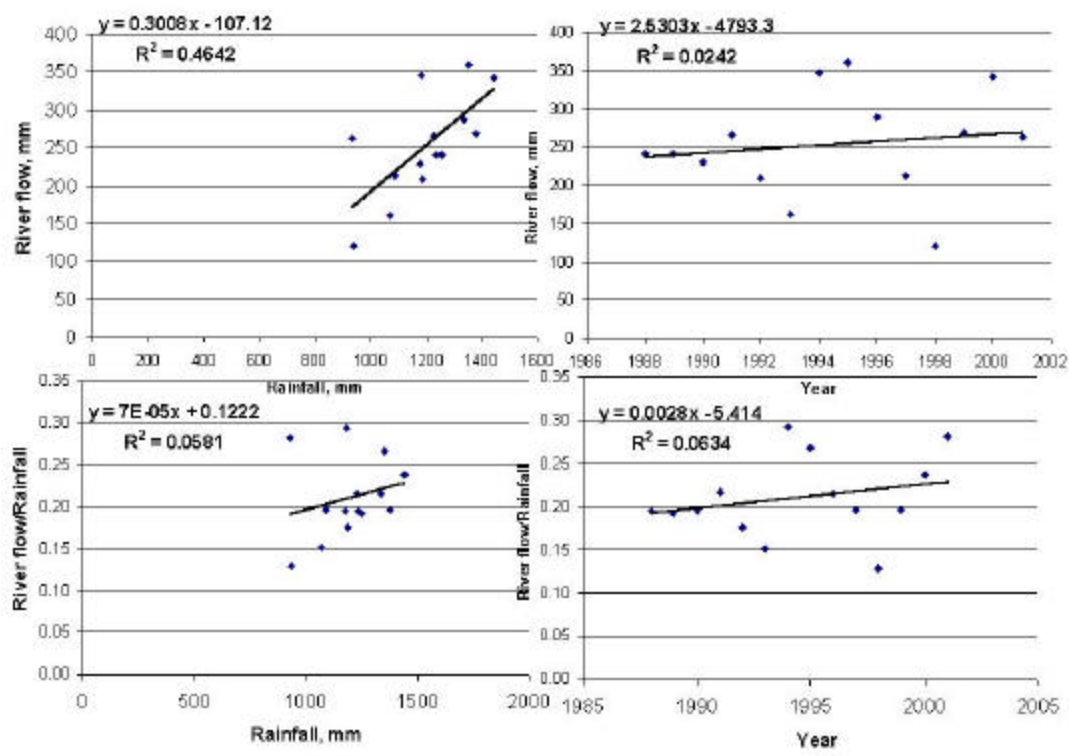


Figure 3.2. Relationship between annual discharge (upper panels) and discharge per unit rainfall (lower panels) of the Mae Chaem river (P14 station) in relation to annual rainfall (left panels) and year (right panels) for the rainfall recorded at the Mae Chaem town climate station, for the period 1988 - 2000

In the absence of a trend with time, we can pool the data over the period available and look for the frequency distributions of both rainfall and river flow in the form of ‘exceedance’ probabilities (Fig. 3.3 -- compare fig. 1.13)

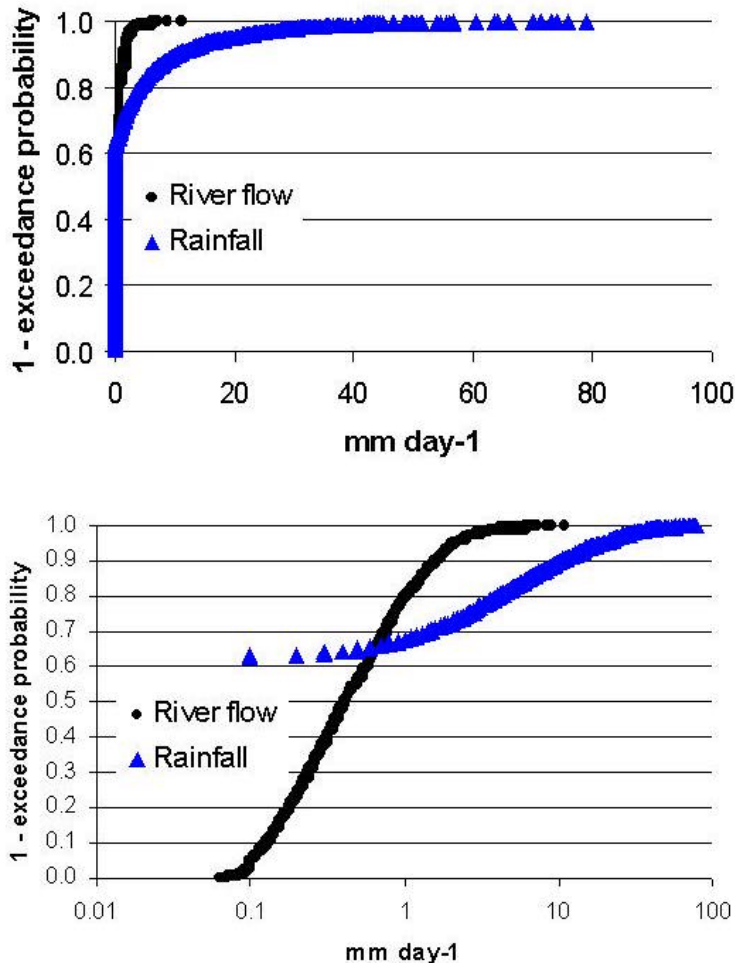


Figure 3.3. Exceedance probabilities for rainfall (Mae Chaem climate station) and river flow data for 1988 – 2001, expressed on linear (upper panel) and logarithmic scale

When presented this way we see that the river flow has a considerably lower maximum and higher minimum, but otherwise similarly shaped distribution. A comparison of the shape of these two curves can lead to us a ‘buffering indicator’. The amount of above-average river flow per unit above-average rainfall may meet both the intuitive concept of buffering and be easy to calculate. As indicated in Figure 1.13, the areas to the left of the rainfall and river flow curves would equal the total amount of water involved, and the difference between these two values would be (approximately) equal to the total evapotranspiration.

For Mae Chaem this buffering indicator (the above-average river flow per unit above-average rainfall) is about 0.95 for the 1988 – 2001 period, and, does not show a clear trend with time or annual total rainfall (upper panels in Fig. 3.4). A direct plot of sorted daily rainfall versus sorted daily river flow indicates a straight line over most of

the range, with a slope of about 0.08, but also a few points exceeding the line that indicates that the days with the highest river flow did not have matching days with high rainfall (lower panel in Fig. 3.4).

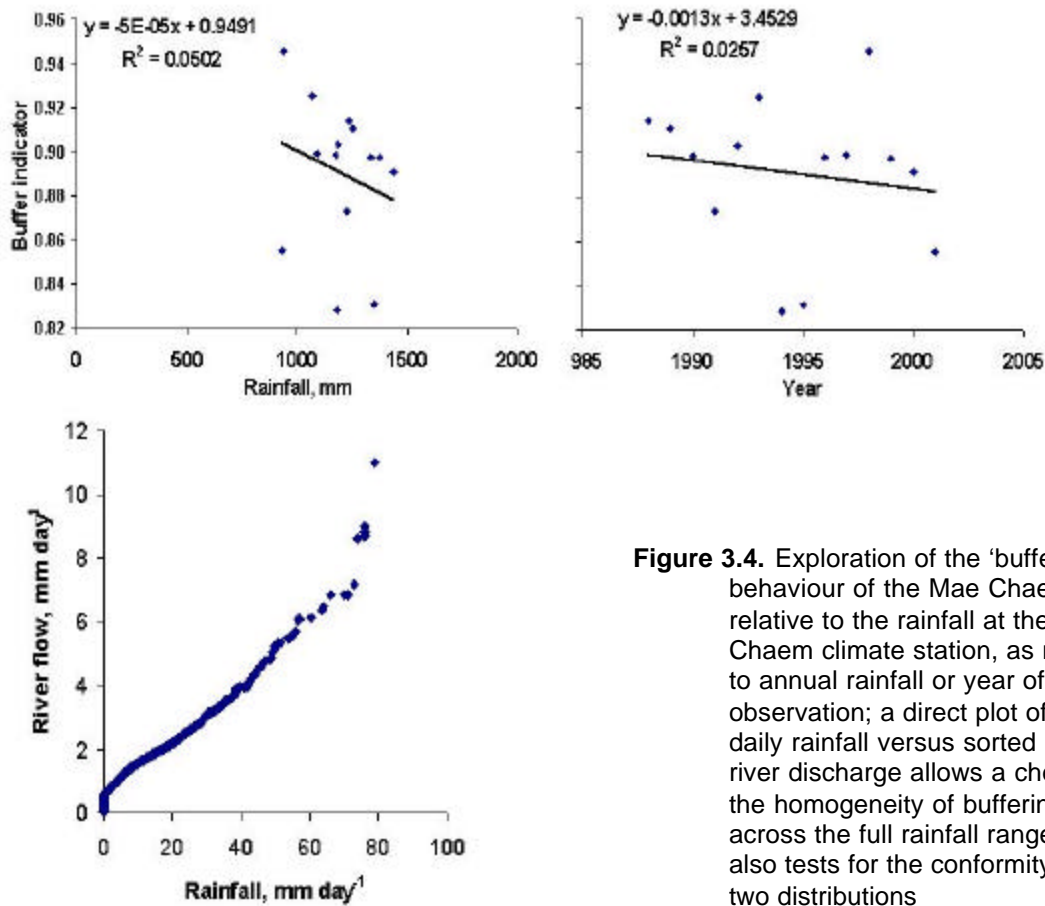


Figure 3.4. Exploration of the ‘buffering’ behaviour of the Mae Chaem river relative to the rainfall at the Mae Chaem climate station, as related to annual rainfall or year of observation; a direct plot of sorted daily rainfall versus sorted daily river discharge allows a check of the homogeneity of buffering across the full rainfall range; it also tests for the conformity of the two distributions

3.1.3. Seasonal effects on buffering in Mae Chaem

The difference that was noted in the discussion on Fig. 3.1 on the difference between the first and second half of the rainy season was further explored by analysing the frequency distributions of rainfall and river flow for four quarters of the ‘hydrological year’, based on equal expected values for rainfall.

The results for the 1st and 2nd quarter of the annual rainfall year in Fig. 3.5 clearly differ from those for the 3rd and the 4th quarter, with the greatest transfer of rainfall to river flow for period 3 (which lasts little over a month). This pattern is consistent with a build up of soil water deficit during the dry season (1st quarter), recharge during 2nd quarter and rapid transfer to the river in the 3rd quarter when the soil stays close to field capacity.

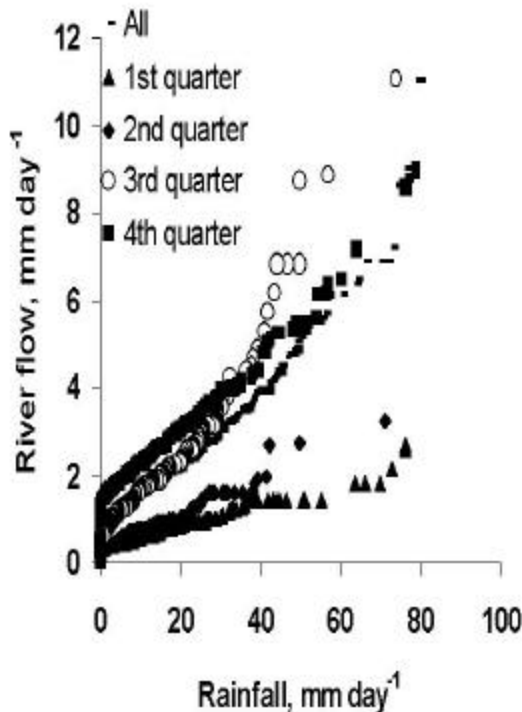


Figure 3.5. Relationship between rainfall and river flow distributions for four quarters of the hydrological year in Mae Chaem that each represent one quarter of the annual rainfall: January 1st – June 4, June 5th – July 27, July 28th – September 1, September 2nd – Dec 31, respectively

3.1.4. Exploration on orographical effects on rainfall in Mae Chaem

The long-term climate station at Mae Chaem town is in the lower part of the catchment, and is unlikely to fully represent the catchment as a whole. Preliminary exploration of elevational and orographic effects on space-time patterns of rainfall was done using 2-year full datasets (1998-1999) of daily rainfalls as recorded by 13 stations in Mae Chaem, obtained from GAME-T Project (Table 3.1). In this analysis, we assigned one station as the reference (POU station at Mae Chaem, for which long term records are available). We use relative rainfall (R_r) and altitude difference (dZ), which are relative values to the reference, to study the elevational effects in Mae Chaem.

In this exploration, we consider both seasonal patterns – linked to dominant wind directions – and aspects of terrains toward the wind direction. In Mae Chaem, we recognized 2 main parts of the wet seasons, driven by southwest monsoon in April-September period and northeast monsoon in October-March period (Figure 3.5). Based on the DEM of the area using grid resolution of 1 km^2 , 13 stations used in this study are located on terrains with dominant aspects toward northwest, southeast and southwest.

Table 3.1. Rainfall stations in Mae Chaem used for this study (rainfall data obtained from GAME-T Project).

No	Station	Aspect	Elevation (m a.s.l.)
1.	Ob Luang	NW	380
2.	Sirikit Plantation	NW	1330
3.	Mae Ning	NW	1630
4.	Mae Sa	SE	650
5.	Research Station	SE	1100
6.	Mae Yod	SE	1180
7.	Bo Kaeo	SE	1400
8.	Mae Klang	SE	1540
9.	Doi Inthanon	SE	2565
10.	POU	SW	490
11.	Wat Chan	SW	990
12.	Mae Long	SW	1450
13.	Mae Jon	SW	1470

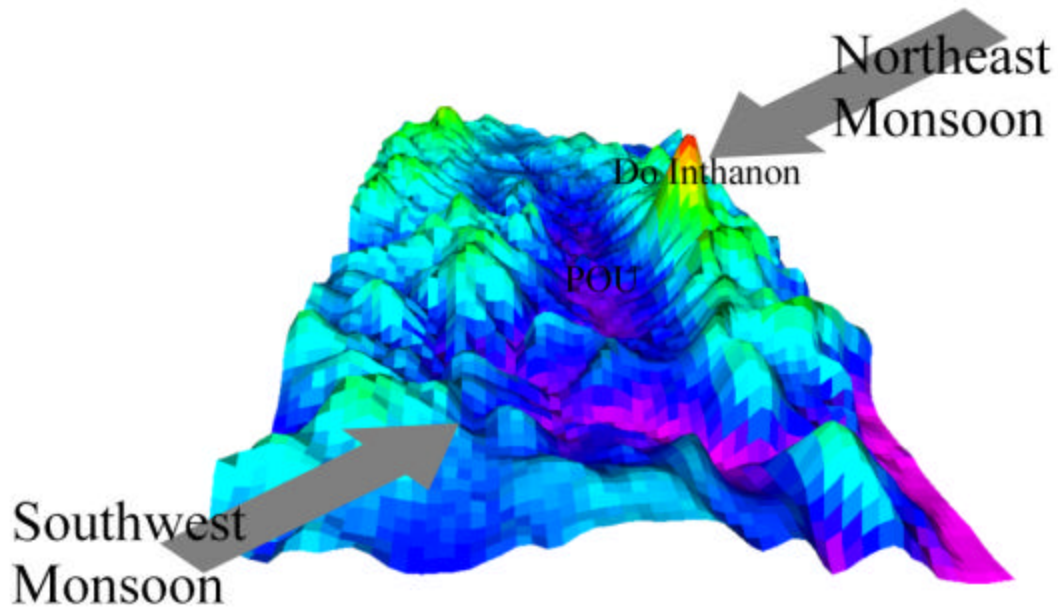


Figure 3.6. Southwest and northeast monsoons, as two main seasons determining dominant wind direction in Mae Chaem. POU is the reference station in Mae Chaem town

When considered at annual time scale, there is considerable spread in the elevational effect (Figure 3.7).

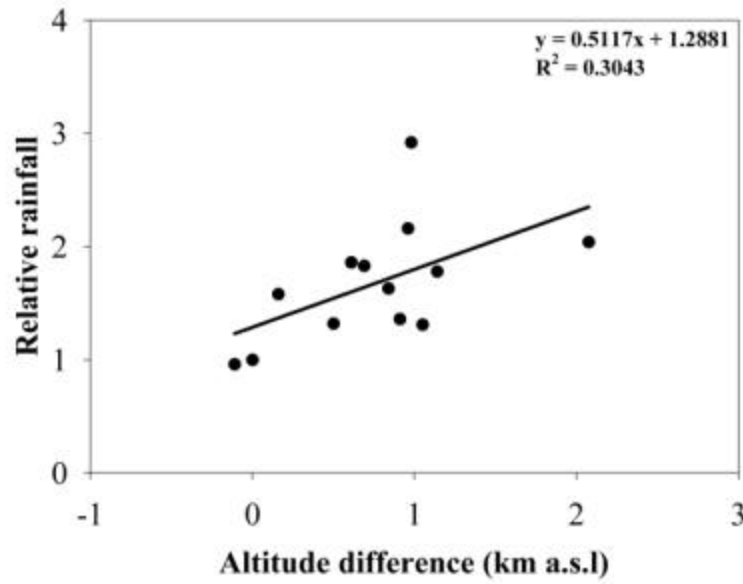


Figure 3.7. Overall relationship between relative annual rainfall total and difference in elevation with Mae Chaem town.

To further explore the elevation effect we split the data by aspect and time of year, based on the monsoon periods (Fig. 3.8). Differences in relative rainfall are larger in the northeast monsoon (values up to 6) than in the southwest monsoon (values up to 2.5). We interpret these results in the light of the position of Mae Chaem town in the 'rain shadow' of Doi Inthanon during the NE monsoon. The overall relationship between elevation and rainfall depends largely on the southwest monsoon, as the slope of the line for the northeast monsoon is close to zero.

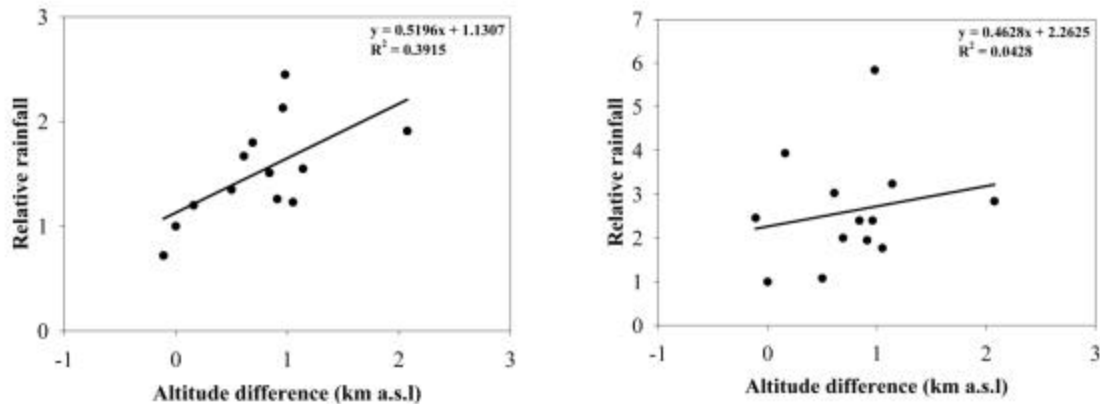
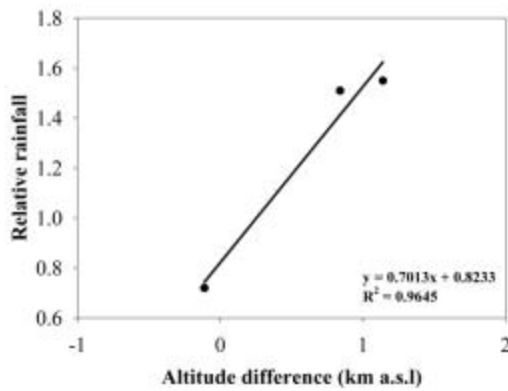
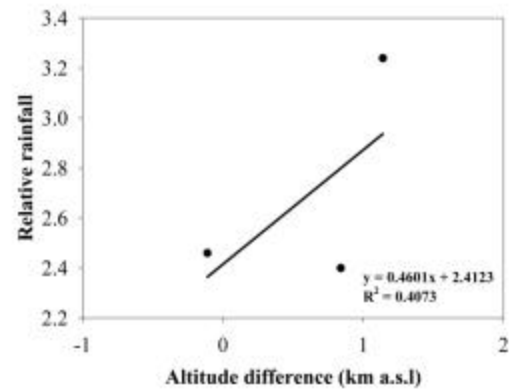


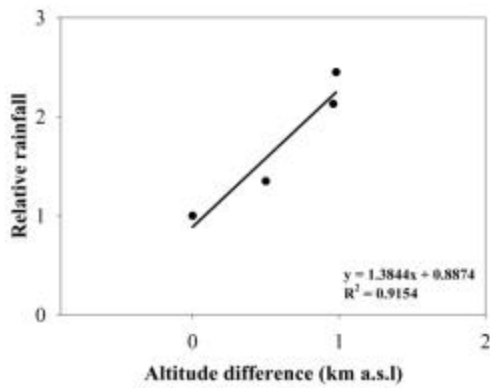
Figure 3.8. Relationship between rainfall (relative to that at Mae Chaem town) and elevational difference from Mae Chaem town for the southwest (left) and northeast (right) monsoon, respectively



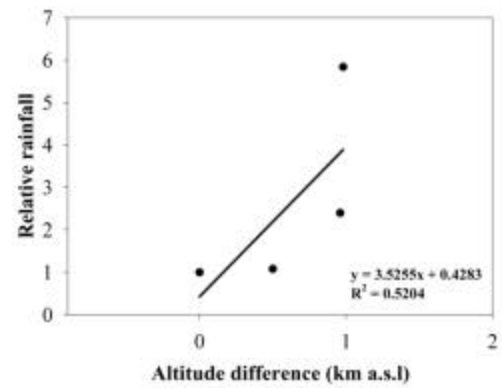
NW aspect against SW monsoon



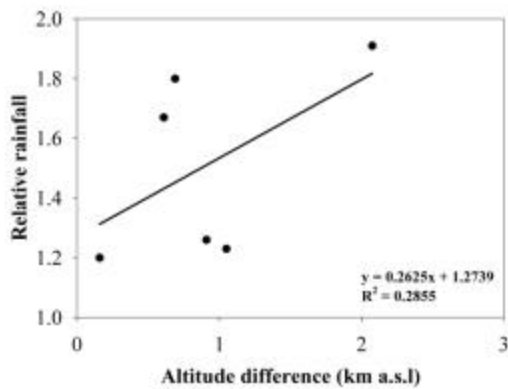
NW aspect against NE monsoon



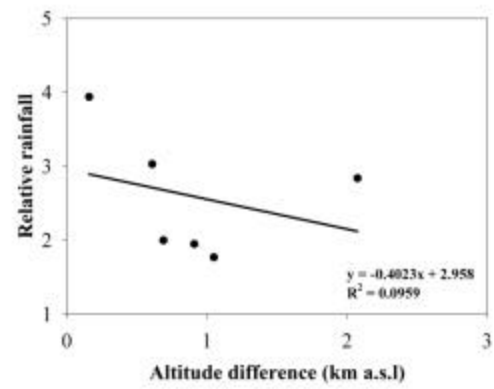
SW aspect against SW monsoon



SW aspect against NE monsoon



SE aspect against SW monsoon



SE aspect against NE Monsoon

Figure 3.9. Relation between elevation and rainfall for the GAME-T rainfall stations in Mae Chaem in the SW Monsoon period (left) and NE Monsoon period (right)

Classification of the rainfall stations by aspect suggests (although the number of points per class is small) that the elevational effect is strong for rainfall stations on positions facing southwest and northwest, but weaker for southeast aspects (Fig. 3.9).

For the northeast monsoon period the relationship between relative rainfall and elevation was weaker defined (lower percentage of variance accounted for by linear regression), but still positive for northwest and southwest aspects. For stations with a southeast aspect the elevational aspect during the northeast monsoon appears to be negative.

In conclusion, the rainfall station with the longest rainfall records is likely to give an underestimate of the rainfall in the catchment as a whole. This may be particularly true for the second part of the rainy season, during the northeast monsoon. During this period, elevational effects are likely to be confounded by ‘orographic’ effects that include rain shadows from the Doi Inthanon peak.

3.1.5 Way Besai river flow data 1975-1998

The primary data for rainfall and river flow in the Way Besai catchment show a seasonal pattern that emerges despite the considerable year-to-year variation (Fig. 3.1). Over the 1975 – 1998 period of the data, the relationship between river flow and rainfall has changed markedly: the ratio of river flow and rainfall has increased from around 0.5 to 0.7 (fig. 3.10). This increase in the relative flow occurred during a period with a negative overall trend in rainfall (Fig. 3.11D). The increase in relative river flow meant that the number of days where river discharge exceeded $25 \text{ m}^3 \text{ s}^{-1}$, the target value in the technical design of the run-off hydro-electricity generator operated by PLTA Way Besai has increased significantly with time (Fig. 3.11 C).

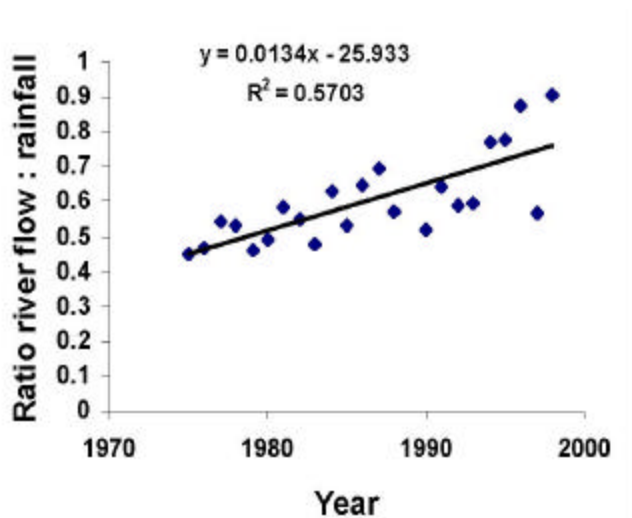


Figure 3.10. Ratio of annual total river discharge and rainfall (both expressed per unit area) for the Way Besai in the period 1975 – 1998

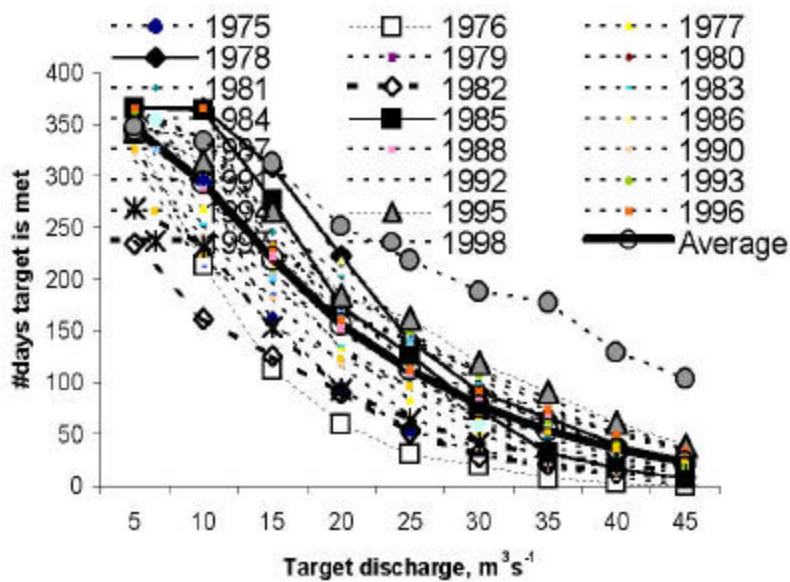


Figure 3.11. Number of days per year that the discharge of the Way Besai exceeds discharges in the range of 5 – 45 $\text{m}^3 \text{s}^{-1}$ (the run-off electricity generator operates at maximum capacity for a daily discharge of 25 $\text{m}^3 \text{s}^{-1}$)

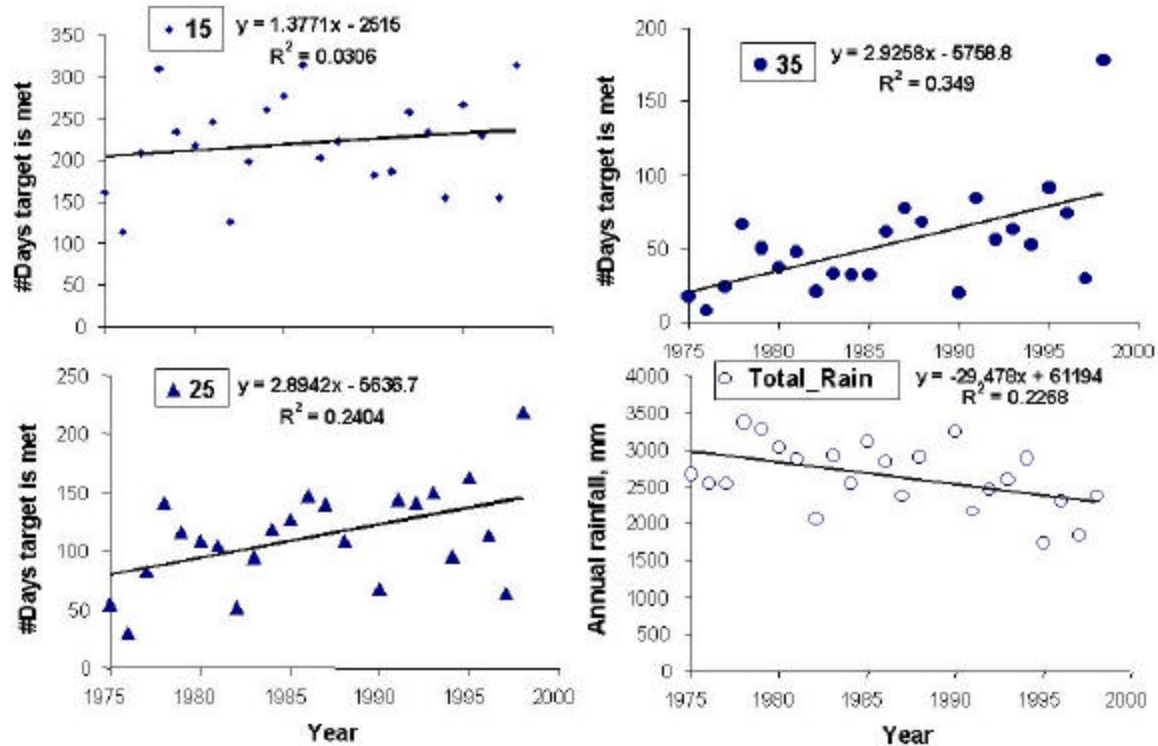


Figure 3.12. Change with time in the number of days that the Way Besai meets a target discharge of 15, 25 or 35 $\text{m}^3 \text{s}^{-1}$, and the annual rainfall over the 1975 – 1998 period

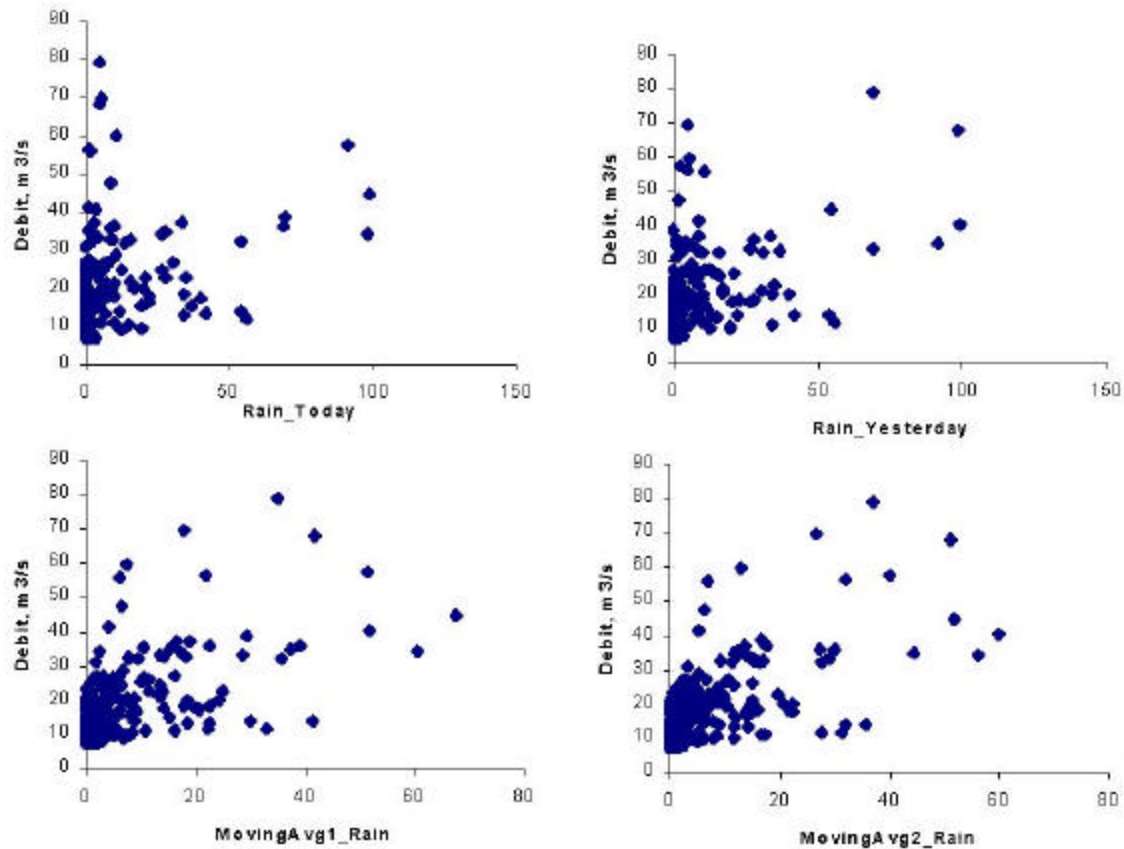


Figure 3.13. Relationships between daily river discharge and rainfall on the same day (A), the day before (B) or a moving average involving the day itself and the two preceding days (with weights of 0.4, 0.4 and 0.2, respectively) (C) or the preceding three days (0.2, 0.4, 0.3, 0.1) (D)

A further analysis of the data and the way river flow responds to daily rainfall is needed, but the direct concern expressed by the PLTA Way Besai of a reduction in the number of days that the turbines will be able to function due to changes in river flow is not supported by the data available.

On a daily basis, however, the relationship between rainfall and river flow is less obvious than it is for the annual total. The response of the river takes some time to appear and to subside after each rainfall event. However, if in figure 3.8 relationships are explored between rainfall on the day itself, rainfall on the day before and two types of moving average (I: 0.4, 0.4, 0.2; II: 0.2, 0.4, 0.3, 0.1, as weights for rainfall on the day itself and the days before, respectively), there is only a slight improvement in the percentage of variance accounted for. A possible explanation for this effect in the form of spatial variability of rainfall will be explored in section 3.4.

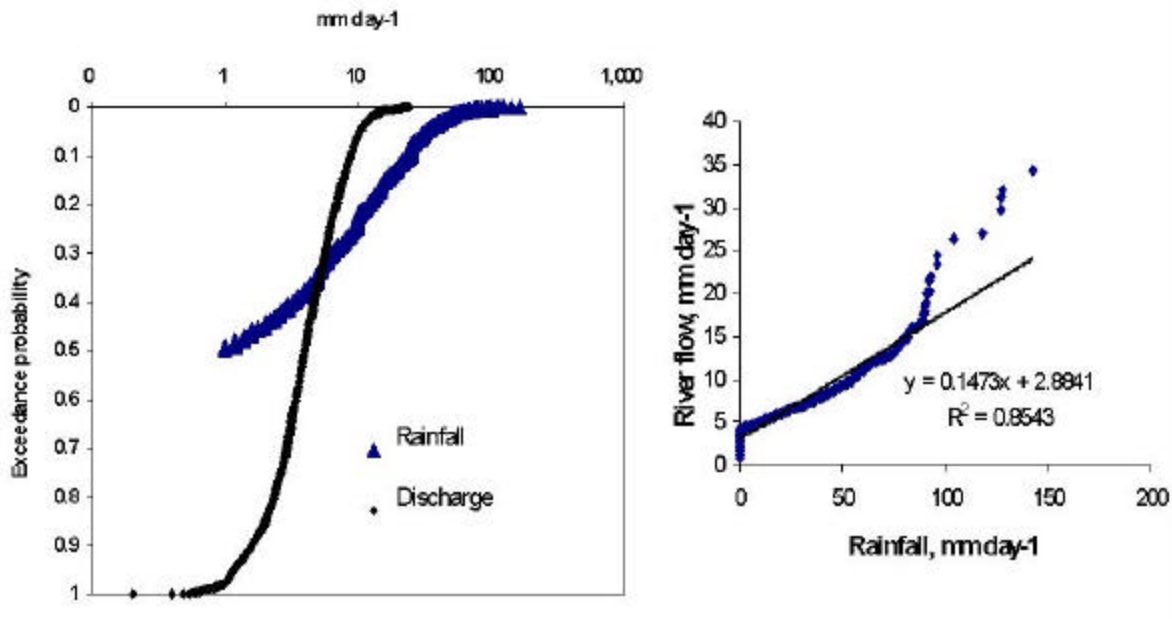


Figure 3.14. Rainfall and river flow exceedance graphs for Way Besai in the period 1975 – 1998

River discharge and rainfall distributions are generally conform, as shown by the vast majority of points that fit on a straight line (Fig. 3.10); the top 15 points (out of a total of 8000 for 22 years), however, deviate from the line. All these points derive from the last 8 years of the time series. By splitting the time series into three parts with 7(+) years each (Fig. 3.11), we can see a gradual shift in slope of the line (consistent with increase in total water yield per unit rainfall). In the last 7 years we see that rainfall events of about 50 mm are associated (in the ranking...) with river discharges that are disproportionately high. For the highest recorded rainfall events, however, the discharge returns to the initial slope of the line.

Our tentative interpretation of these data is that in the 1990's for rainfall events around 50 mm day⁻¹ we see an increase in runoff fraction linked to changes in the soil after the substantial land cover change of the 1980-'s. However, for the highest events, ban overflow in the lower section of the river is an important feature in overall buffering, and this part of the overall buffering is still intact.

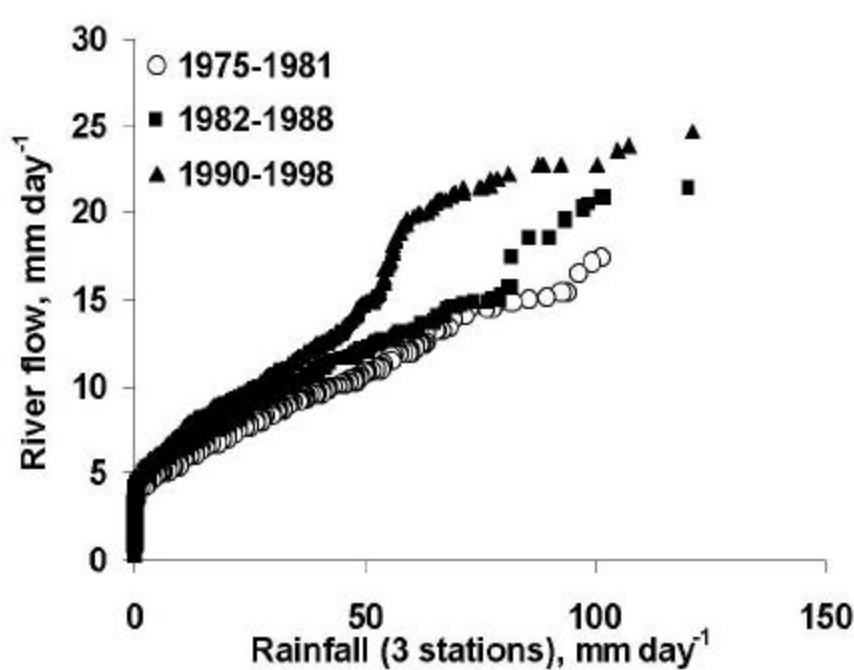


Figure 3.15. Buffer indicator 0.74 for period as a whole (1975-1998) and 0.78, 0.71, 0.62 for the periods 1975-1981, 1982-1988 and 1990-1998, respectively.

Earlier analysis of the hydrographs by Sinukaban et al. (2000) used a peak flow separation technique on data for 5 years with comparable total annual rainfall. Estimates of total evapotranspiration were obtained by subtracting discharge from rainfall total, and indicate a remarkable decrease with time. Both quick flow and base flow (with the operational definitions used in the study) increased relative to rainfall, but the percentage quick flow remained approximately constant at 17 – 22%. This ratio is slightly below what the ‘buffering indicator’ (or its complement) suggests as proportion of flow directly associated with rainfall peaks.

Table 3.2 Water balance Sumberjaya (mm) as derived by Sinukaban et al. (2000)

Component	1975	1980	1985	1991	1995
Rain	2531	2797	2959	2459	2663
Evapo-transpiration	1162	1119	1166	741	662
Quick-flow	237	293	382	374	342
Base-flow	1132	1385	1411	1344	1659
%Quickflow	17	17	21	22	17

3.1.6. Seasonal effects on buffering in the Way Besai catchment

Splitting the hydrological year for the Way Besai into four quarters that each represent one quarter of the annual rainfall total (Fig. 3.16) leads to smaller seasonal difference in buffering than we found for Mae Chaem (Fig. 3.5). The third quarter (which represents the longest period and thus the lowest mean daily rainfall rate), the slope of the relationship between rainfall and river flow is the lowest (highest ‘buffering indicator’)

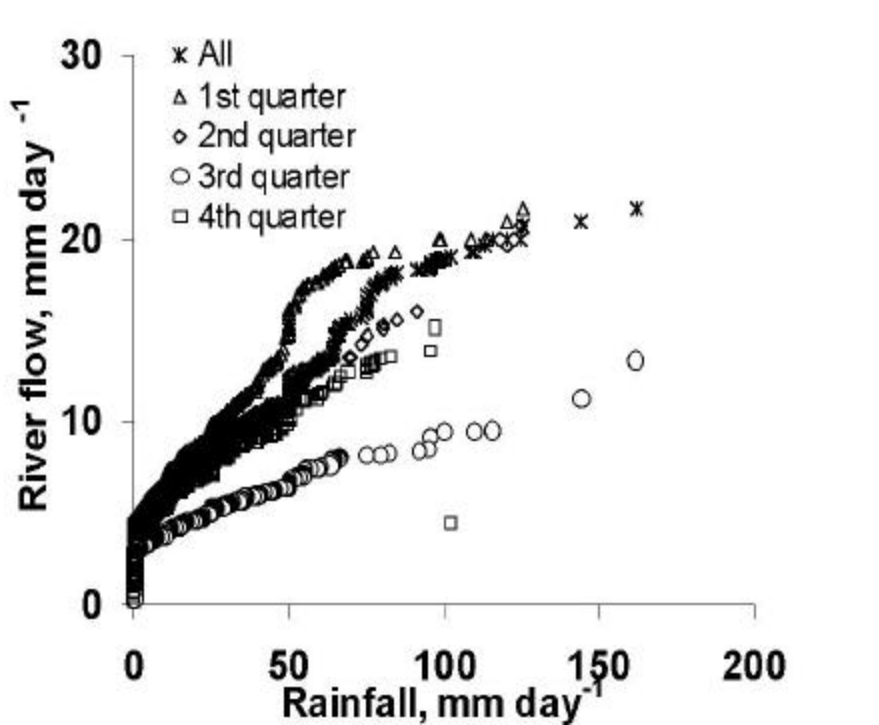


Figure. 3.16. Relationship between rainfall and river flow distributions for four quarters of the hydrological year in Way Besai that each represent one quarter of the annual rainfall: 1 Jan - 11 Mar, 12 Mar - 26 May, 27 May - 17 Oct, 18 Oct - 31 Dec respectively

3.1.7 Spatial rainfall patterns in the Way Besai catchment

All rainfall stations for which measurements exist are in the valley of the Way Besai, with little difference in elevation, so we cannot derive an elevational effect for the Way Besai area. Analysis of the spatial patterns in rainfall for the Way Besai catchment by Manik and Siddle (2003) (Fig. 3.17) shows that inter-station correlation of daily rainfall drops to low values within a distance of 2 km. For monthly totals the correlation declines more gradually with distance to a value of 0.6 at a scale of 20 km (the cross section of the catchment). For monthly totals, however, there is no indication of consistent spatial patterns within the catchment, so we ascribe the low correlation to a strongly patchy process of rainfall in storms.

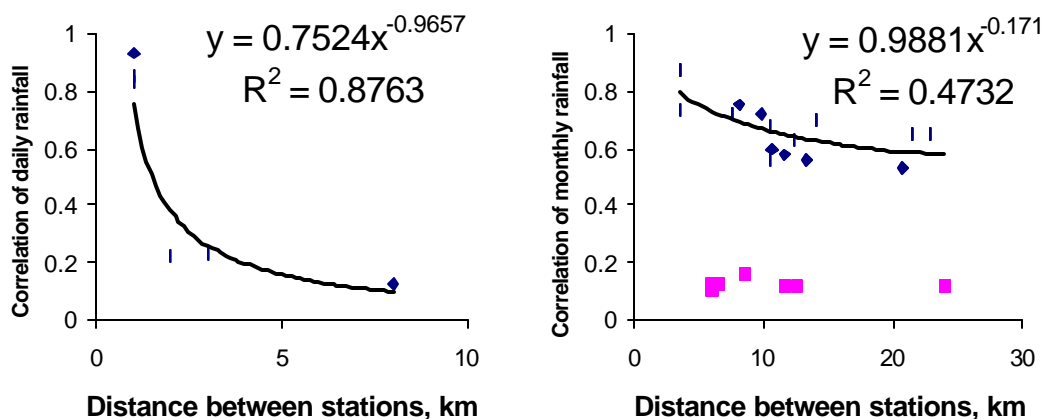


Figure 3.17. Decrease of inter-station correlation of daily (left) and monthly (right) rainfall for the Way Besai catchment (Sumberjaya, Lampung, Indonesia) of the Tulang Bawang river; data for one station indicated by the squares showed very little correspondence with any of the others, and was left out of the regression line (based on: Manik and Siddle, 2003)

3.2 Hydrologic null-model of a forest conversio- degradation–rehabilitation cycle

Results for the null-model give an ‘order-of-magnitude’ representation of the possible longer-term changes in the water balance under the impacts of land use change. The null-model ignores most of the dynamic interactions between terms of the water balance, but does indicate a key trade-off in land cover change: changes in aboveground water use by vegetation and changes in the partitioning of rainfall over quick and slow flow pathways.

3.2.1 Step 1: removing forest cover increases total water yield of the catchments

Removing forest cover is likely to reduce the amount of water intercepted and/or used by the vegetation, to the tune of 300 mm year^{-1} . In the absence, initially, of changes in soil structure and infiltration capacity, most of this extra water may come as slow flows, except when saturation effects cause an increase in the runoff fraction (Fig. 3.18).

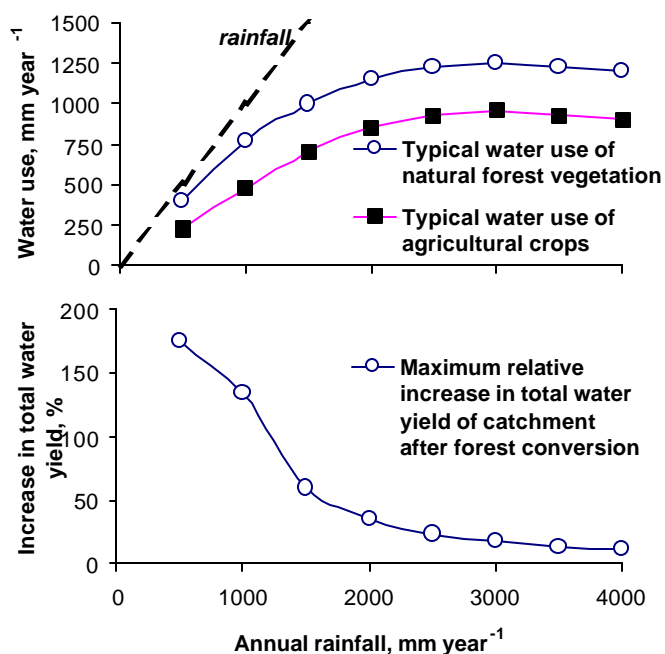


Figure 3.18. A. Natural forests typically use more water than open-field agriculture (with most other land uses intermediate); B. Removal of the forest vegetation will increase the total water yield, but the relative increase depends on annual rainfall

3.2.2 Step 2: increase in runoff increases peak flow and reduces base flow

After forest conversion to other land use, a stepwise degradation of soil structure may be expected, that will lead to a shift from slow flows to quick flows, at constant total water yield (Fig. 3.19). An initial increase in slow flows will be offset by greater runoff.

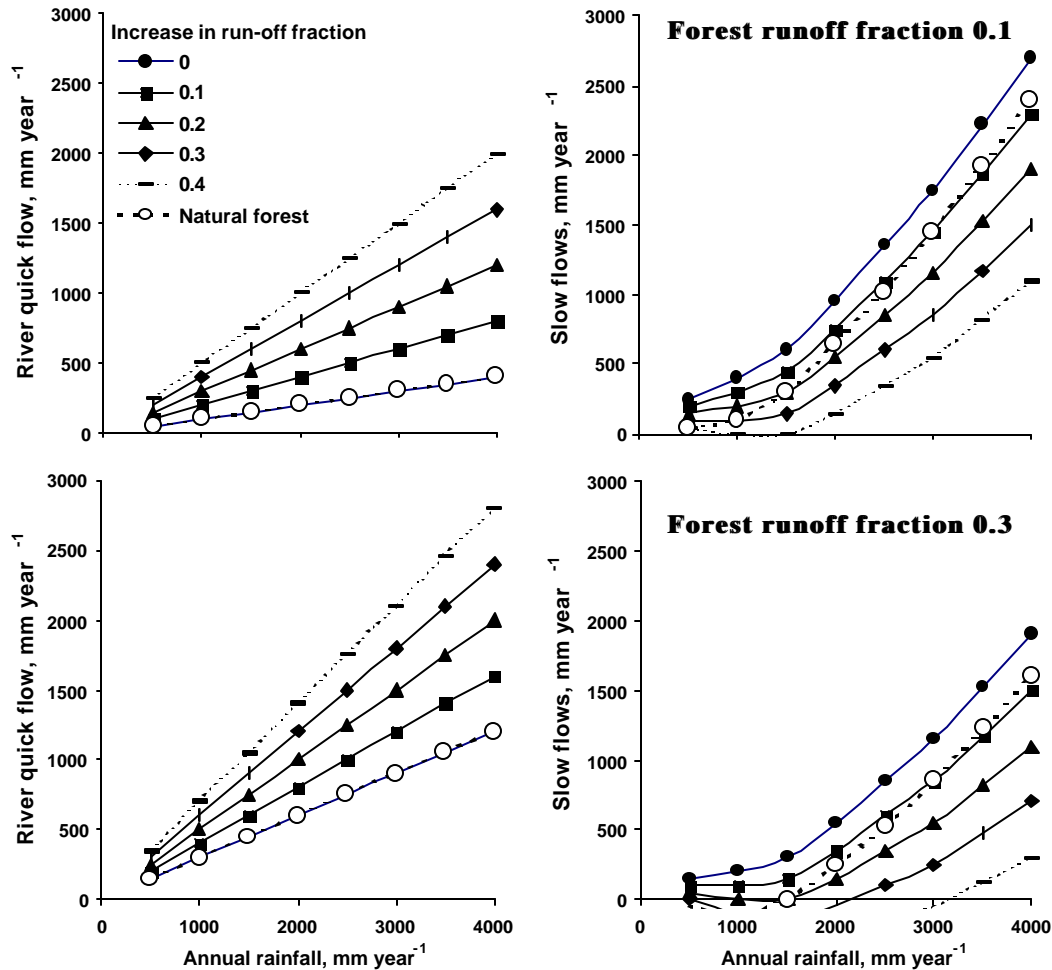


Figure 3.19. River quick flow and slow flows as a function of annual rainfall as affected by a change from natural forest to open-field agriculture, for a range of impacts on the run-off fraction (upper two graphs for a forest run-off fraction of 0.1; lower two graphs for a forest run-off fraction of 0.3, typical for steeper terrain, shallower soils and/or more intense rainfall)

Regardless of the runoff fraction under forest condition the break-even point for slow flows is obtained in the situation where the reduction in water use equals the increase in run-off fraction times the annual rainfall. For our numerical example: at 3000 mm year⁻¹ for an increase in run-off fraction of 0.1, at 1500 mm year⁻¹ for an increase in run-off fraction of 0.2, at 1000 mm year⁻¹ for an increase in run-off fraction of 0.3 or at 750 mm year⁻¹ for an increase in run-off fraction of 0.4.

3.2.3 Step 3: Reforestation causes a decrease in total water yield and base flow

In the landscape rehabilitation phase, when tree cover increases, we can expect a relatively fast increase of total water use and a slow recovery of infiltration (reduction of the run-off fraction))

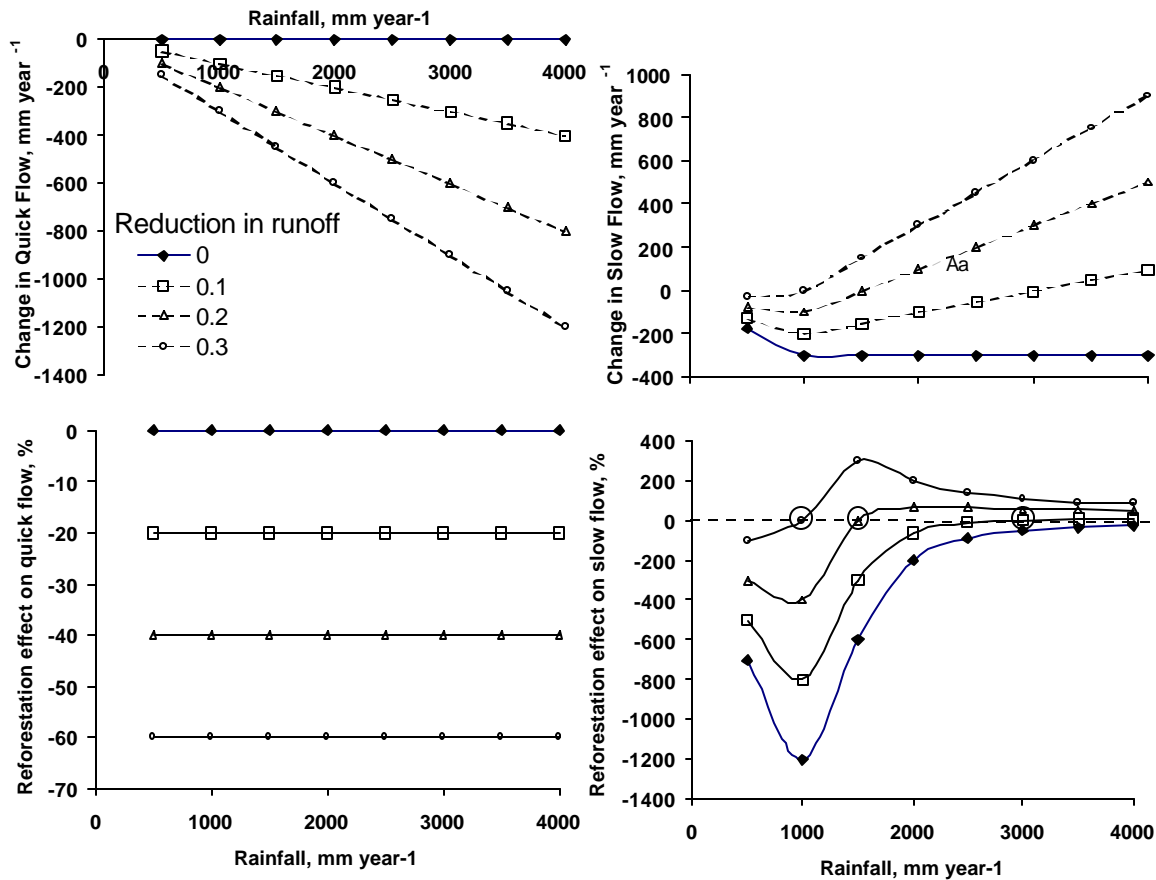


Figure 3.20. Expected changes in absolute and relative quick flows and slow flows in response to reforestation and a subsequent reduction in run-off fraction, for a situation where the run-off fraction had increased to 0.45 and the increase in water use is approximately 300 mm year⁻¹; circles indicate 'break-even' points where negative impacts of reforestation on slow flows turn into positive effects, depending on the reduction in the runoff fraction

Reforestation can always be expected to reduce quick flow in the river and total water yield, but the impact on slow flows depends on the decrease in run-off fraction; the break-even point again is based on the difference in total water use, total rainfall and the change in run-off fraction, with a neutral effect at a rainfall of 3000 mm year⁻¹ for a change in runoff fraction of 0.1, at a rainfall of 1500 mm year⁻¹ for a change in runoff fraction of 0.2 or at a rainfall of 1000 mm year⁻¹ for a change in runoff fraction of 0.3.

For all three phases of the process we see that changes in the run-off fraction, and the degree of reversibility of soil degradation, are of crucial importance.

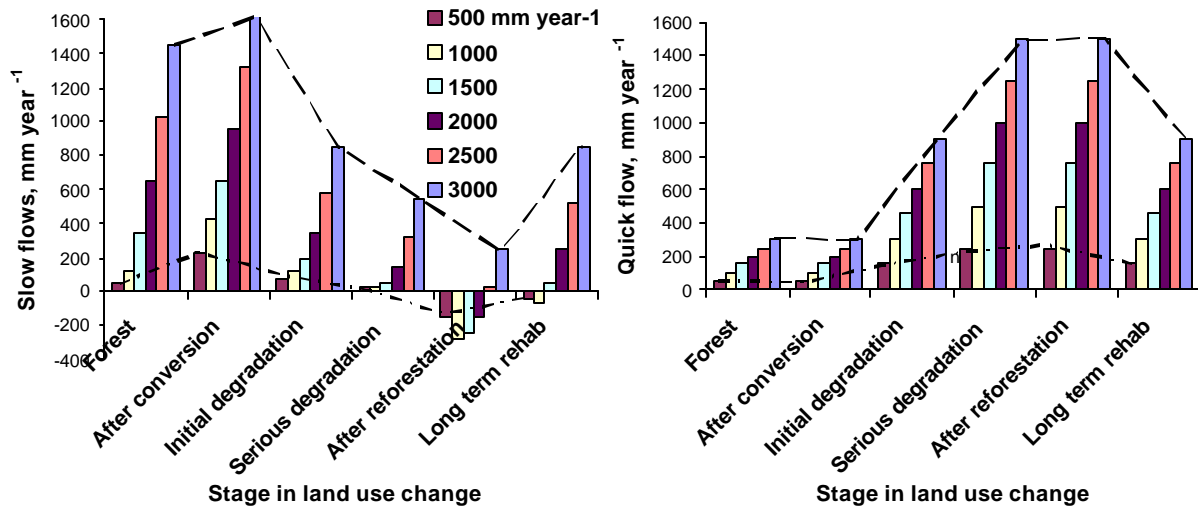


Figure 3.21. Cross section of changes in slow flows and quick flows across a land use change trajectory, assuming an increase in the run-off fraction of 0.2 and 0.4 during the initial and serious degradation phase, and a recovery of 0.2 during long-term rehabilitation; negative estimates of 'slow flows' indicate values of zero with likely limitations to tree water use and growth

In looking at the net effect of a change in land cover on 'slow flow' (i.e. flow through pathways other than overland flow -- admittedly part of this can be 'soil quick flow'), we need to offset the difference in total water use (generally of the order of 300 mm year^{-1} or less, except for rainfall patterns that lead to very high interception losses) against the difference in amount infiltrating. A simple calculation shows that for annual rainfalls of $1000 \text{ mm year}^{-1}$, this requires a change in effective infiltration of 30% of the rainfall (so e.g. from 40% runoff to 10% runoff), at $1500 \text{ mm year}^{-1}$ a change of 20% and at $3000 \text{ mm year}^{-1}$ a change of 10%. With negative changes of 20% easily feasible under soil degrading and runoff-facilitating land use change, we can expect a negative impact on soil-infiltration-dependent river flow for forest conversion at $1500 \text{ mm year}^{-1}$ or higher, but see that at rainfall amounts less than $1000 \text{ mm year}^{-1}$, a strong degradation is needed before we expect negative effects on dry-season flows. This simple calculation also shows that 'rehabilitation' hinges on substantial changes in effective infiltration rates, with the increase in total water use usually more rapid than a change in soil structure and net infiltration.

The 'null-model' thus shows that an internally consistent representation of the hydrological impacts of land cover change can treat changes in total water use and changes in the run-off fraction as operating at different time scales. The aboveground changes, probably directly linked to a major part of biodiversity, but only accounting for effects on total water yield, not for its partitioning over slow and quick flows, can occur considerably faster than the changes in soil structure that dominate runoff. Again, this points towards a considerable decoupling of biodiversity conservation and watershed function issues.

Progress over and beyond the null-model will hinge on a better understanding of the changes in the run-off fraction that can be causally linked to forest conversion, degrading practices and rehabilitation efforts.

3.3 WaNuLCAS analysis of changes in infiltration after forest conversion

3.3.1 Comparing lateral flow modules of the FUSSIM and WaNuLCAS models

The WaNuLCAS as well as GenRiver model operate on a daily time step, while the dynamics of infiltration of rainfall into soil may change at a minute or even second time scale, depending on variation in rainfall intensity during storms and the impact of changing soil water content on the capacity of the soil to absorb and transport water. The hydraulic conductivity depends strongly on soil water content. To test the validity of the approach we take at a daily time stop, we compared WaNuLCAS with the detailed soil physical model FUSSIM, for a wide range of soil textures, for a unit of land with a slope of 15-90%. Both models use the same basic representation of soil water retention, so the main degree of freedom for deviation is in the allocation of out flowing water over lateral (overland and subsurface) and vertical pathways, and in the change in lateral flow fraction within the unit of land considered.

Both models predict an increase in lateral flow with increase in slope (Fig. 3.22), but they differ in the relative importance of position on the slope. Increments in lateral flow fraction estimates from the lower to higher position on the slope are larger in WaNuLCAS than in the FUSSIM simulations. Soil texture appears to be relatively unimportant in the prediction of lateral flow, probably because conductivity in horizontal and vertical directions changes proportionally in both models. In WaNuLCAS the effect of texture is almost constant, with a slight increase for clay soils. In FUSSIM the effect of texture is curvilinear, with a decrease for clay soils. A different performance between the two models occurs mainly for clay content higher than 60%. This is due to a difference in the basic assumption. WaNuLCAS calculates soil water content on a daily basis and the maximum soil water content is at field capacity. Any water beyond field capacity would be channeled through vertical flow (drainage) or horizontal flow (lateral flow). Lateral flow is a uni-flow (water can only flow downwards). In FUSSIM soil water content is calculated at finer step (may be 10^{-5} day), where soil water content may reach saturation. A bi-lateral flow occurs, enabling water to move upwards ('capillary rise') as well as downwards. Capillary rise occurs mainly in clay soils.

We can conclude that the relatively simple WaNuLCAS approach in modeling lateral flow is feasible in sandy and sandy-loam soils, but that predictions in clay soils have to be interpreted cautiously.

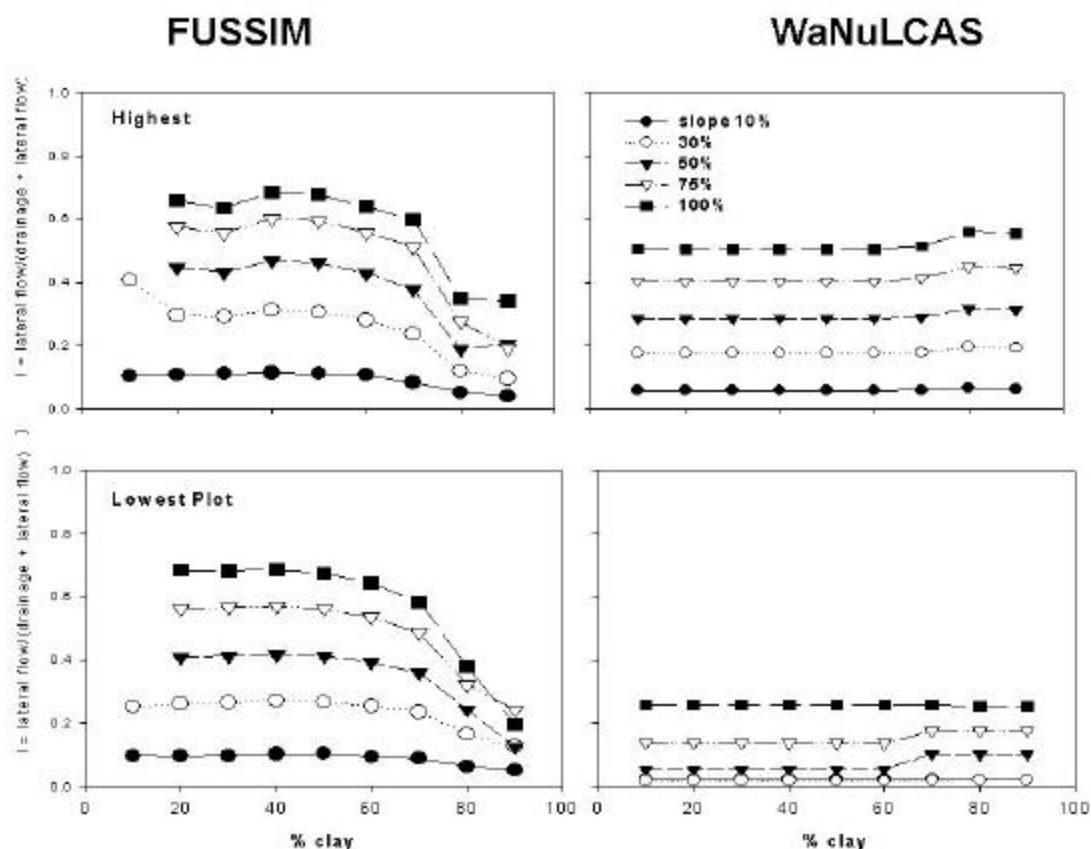


Figure 3.22. Result of WaNuLCAS and FUSSIM simulation on lateral flow

Table 3.3. Slope (a) and percentage of variation accounted for (R^2) of regression equation of **daily values** ($Y_{PTF} = a Y_{PTFRDB}$) for a 10 year WaNuLCAS simulation of a tree-maize system, based on actual field measurements for 6 soils or estimates derived from the P_{TFRDB} database; for maize yield the equation used was $Y_{PTF} = a + b Y_{PTFRDB}$. Slope parameters > 1.2 or < 0.8 , and R^2 values < 0.8 are printed in bold.

	Vertisols		Inceptisols		Alfisols		Mollisols		Ultisols		Entisols	
	a	R^2	a	R^2	a	R^2	a	R^2	a	R^2	A	R^2
θ_{0-100}	1.15	0.86	0.92	0.79	1.11	0.97	1.10	0.96	0.95	0.99	1.22	0.49
ET-maize	1.02	0.94	0.97	0.99	1.00	0.99	1.02	0.99	0.99	0.99	1.00	0.99
ET-tree	0.99	0.66	1.15	0.61	1.05	0.80	0.94	0.81	0.99	0.82	0.84	0.53
E-soil	1.01	0.67	0.81	0.73	0.89	0.86	1.07	0.81	0.98	0.88	1.27	0.97
E-interception	1.02	0.99	0.98	0.98	0.99	0.99	1.01	0.99	0.98	0.99	0.97	0.99
Runoff	0.76	0.90	0.92	0.96	1.04	0.99	1.00	0.99	0.97	0.99	0.95	0.99
Drainage	1.29	0.71	0.86	0.90	0.93	0.98	1.00	0.99	1.03	0.99	1.08	0.97
Lateral Flow	1.16	0.58	0.76	0.72	0.85	0.96	1.09	0.99	1.07	0.98	1.22	0.95
Maize yield	a	0.68	.	0.45	.	0.55	.	0.08	.	0.01	.	0.77
	b	0.92	0.89	0.88	0.98	1.12	0.94	1.01	0.98	0.98	0.98	0.72
Wood yield		1.15	0.96	0.92	0.79	1.11	0.97	1.10	0.96	0.95	0.99	1.22

3.3.2 Validity of pedotransfer function

As discussed in more detail by Suprayogo et al. (2003), in the WaNuLCAS simulations based on the pedotransfer functions, differences between soil types were simulated consistently, although on various soil types one or more of the processes of the water balance appeared to vary with the way input parameters were derived. For crop yields, tree wood production and cumulative water balance terms, however, these impacts were small, with the largest consistent difference in the partitioning between surface runoff and vertical drainage on the vertisol.

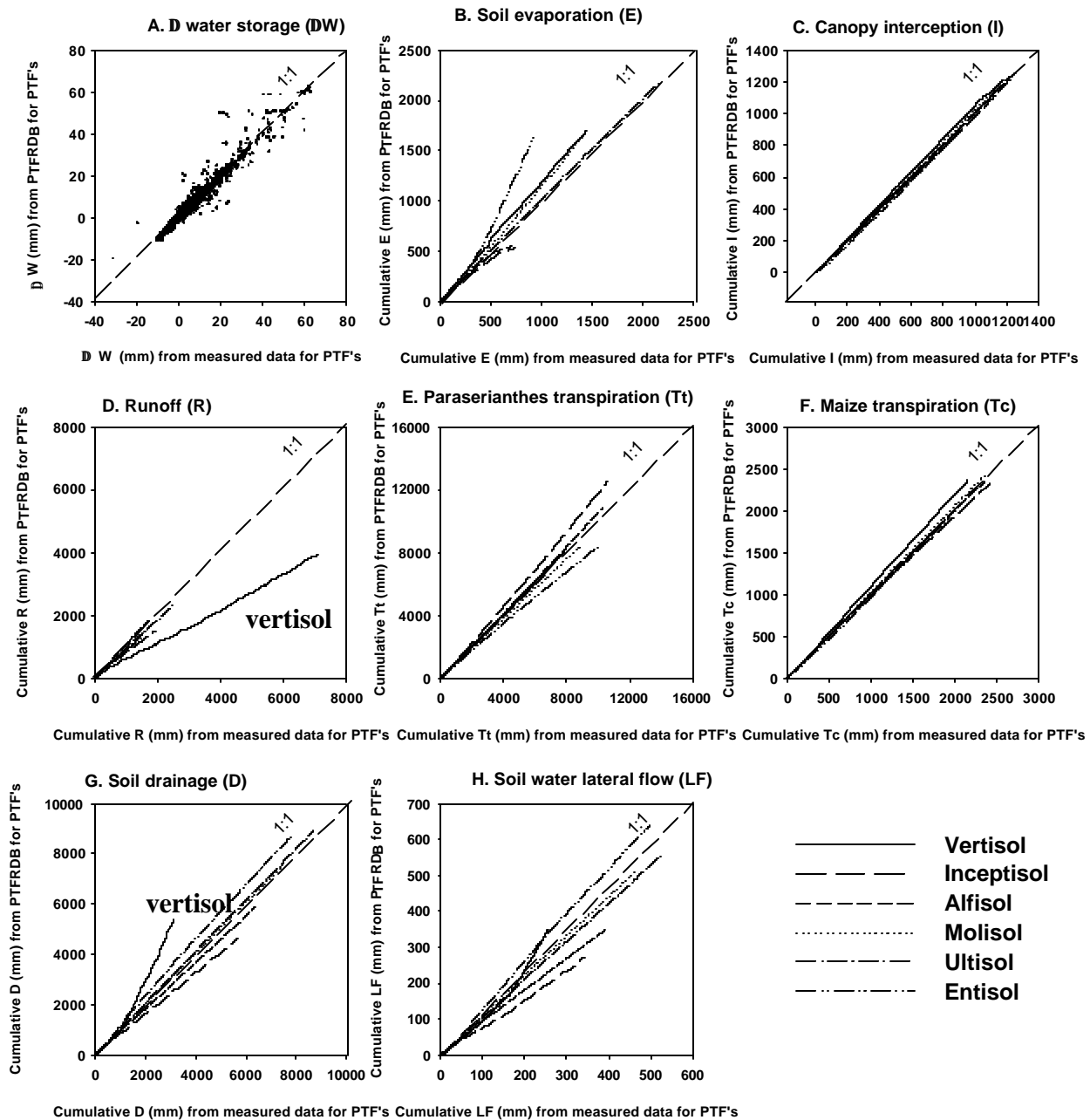


Figure 3.23. Cumulative effects on the terms of the plot-level water balance, for the simulations of Table 3.3